ELSEVIER

Chemical Engineering Journal 137 (2008) 72–83

Chemical Engineering Journal

www.elsevier.com/locate/cej

Nanostructured poly(vinyl alcohol)/bioactive glass and poly (vinyl alcohol)/chitosan/bioactive glass hybrid scaffolds for biomedical applications

Herman S. Mansur *, Hermes S. Costa

Department of Metallurgical and Materials Engineering, Laboratory of Biomaterials and Tissue Engineering, Federal University of Minas Gerais, R. Espírito Santo 35, CEP 30160-030, Belo Horizonte, Brazil

Received 18 June 2007; received in revised form 20 September 2007; accepted 21 September 2007

Abstract

Bone tissue engineering is the field of intense research for developing new 3D scaffolds with hierarchical and highly interconnected porous structure, which should match the properties of the tissue that is to be replaced. These materials need to be biocompatible, ideally osteoinductive, osteoconductive and mechanically well-matched. In the present study, we report the development and characterization of novel hybrid macroporous scaffolds of poly(vinyl) alcohol (PVA)/bioactive glass (BaG) through the sol–gel route. The organic–inorganic hybrids with three concentrations of PVA (80, 70 and 60 wt%) and bioactive glass ($58SiO_2$–$33CaO$–$9P_2O_5$) were synthesized by foaming a mixture of polymer solution and bioactive glass via sol–gel precursor solution. PVA with two degree of hydrolysis, 98.5% (high degree) and 80% (low degree) was also investigated, in order to evaluate the influence of residual acetate group present in polymer chain on the final structure and properties of 3D porous nanocomposites produced (PVA/BaG). Bioartificial polymeric hybrids were also investigated in this work by blending PVA with chitosan (chi) and then reacting with bioactive glass reagents using sol–gel processing route (PVA/Chi/BaG). The microstructure, morphology and crystallinity of the hybrid porous scaffolds were characterized through synchrotron small-angle X-ray scattering (SAXS), X-ray diffraction (XRD), fourier transform infrared spectroscopy (FTIR) and scanning electron microscopy (SEM) analysis. In addition, mechanical properties of hybrids were evaluated by uni-axial compression tests. Biocompatibility, cytotoxicity and cell viability assays were also performed by the MTT method with VERO cell culture. The results have given strong evidence that both hybrid systems of PVA/bioactive glass and PVA/chitosan/bioactive glass were successfully produced and extensively characterized with hierarchical macroporous 3D structure. FTIR spectroscopy associated with XRD and SAXS has proven to be important technique for investigating the formation of PVA/BaG and PVA/Chi/BaG hybrids as organic–inorganic network at micro-nanostructure order. Finally, the developed hybrids have presented suitable mechanical, morphological and cell viability properties for potential biological applications.

Keywords: Hybrids; Bioceramic scaffold; Nanocomposite; Bioactive glass; Polyvinyl alcohol; Bone tissue engineering; Cytotoxicity

1. Introduction

Regenerative biology promises to be one of the biomedical revolutions of the current century. It includes three research approaches: implantation of bioartificial tissues, cell transplantation and stimulation of regeneration from residual tissues *in vivo*. For that reason, nanoscience and nanotechnology will certainly be of paramount importance for assisting researchers to explore the interfaces of living tissues and biomaterials. The past three decades have already witnessed a tremendous increase in the use of biomaterials for bone related surgical applications [1–9]. However, a gap remains to be filled since no synthetic material used until now presents characteristics close to the natural tissue, attending both biological aspects as well as mechanical requirements. Among these materials, bioactive ceramics have been largely studied and used due to their properties of hosting bone cells and the ability of promoting the formation of a continuous bone–ceramic interface, therefore allowing an implant fixation mechanism. Bioceramics usually have mechanical properties quite different from those of natural tissues, particularly a high elastic modulus and a low toughness. Bioactive glasses are important bioceramic materials and have been used for the

* Tel.: +55 31 3238 1843; fax: +55 31 3238 1815.
E-mail address: hmansur@demet.ufmg.br (H.S. Mansur).

1385-8947/$ – see front matter © 2007 Elsevier B.V. All rights reserved.
doi:10.1016/j.cej.2007.09.036

repair and reconstruction of diseased bone tissues [6–11]. These so-called bioactive glasses promote bone tissue formation at their surface and bond to surrounding tissue when implanted in the living body. A common characteristic of bioactive materials is the formation of an apatite-like layer on their surface when they are in contact with physiological fluids or solutions that mimic human plasma [6–12]. Nevertheless, bioactive glasses usually have low mechanical properties, especially in a porous form, compared to cortical and cancellous bone [9–12]. This fact restricts the use of these materials in a wide range of applications. One alternative that is being considered and studied is the production of composites and hybrid systems. Hence, the development of organic–inorganic (O–I) hybrids is regarded as a promising approach for preparing bioactive scaffolds [12–15]. Composites, which include synthetic and biological polymers with a bioactive glass phase, have the potential capability of combining bioactive behavior with adequate mechanical properties. More specifically, composite materials based on biodegradable polymers associated with inorganic bioactive glasses are of particular interest to engineer scaffolds because they offer an excellent balance between strength and toughness and also improve mechanical properties when compared to their individual components [11–17]. These compounds can be synthesized through a hybridization route, in which two different components, namely organic and inorganic, are combined. Sol–gel technology allows the incorporation of polymers of different nature into an inorganic silica bulk, thus producing organic–inorganic hybrid materials [11–13]. Depending on the strength of the interaction between the two phases, the hybrids can be divided in two classes. The first one includes weak-bound components involving hydrogen or van der Waals interactions, whereas the second class of hybrids is characterized by strong covalent bonds [18]. Among several choices of polymers, poly(vinyl alcohol) (PVA), a water-soluble polyhydroxy polymer, has been frequently explored as an implant material in biomedical applications such as drug delivery systems, dialysis membranes, wound dressing, artificial skin, cardiovascular devices and surgical repairs because of its excellent mechanical strength, biocompatibility and non-toxicity [14,15,17,19]. PVA is considered as a biologically friendly material but with some reduced integration to living tissues due to its relative limited biodegradability and bioactivity, compared to poly(ethylene oxide) (PEO), poly(lactic-co-glycolic acid) (PLGA) and others. Therefore, it is promising to blend PVA with biopolymers such as chitosan (chi) to produce a new polymeric system applicable for a variety of purposes [20]. In order to overcome the limited biological performance of synthetic polymers and to enhance the mechanical characteristics of biopolymers, a new class of specially designed materials, 'bioartificial polymeric materials', has been introduced [20–22]. These materials based on blends of both synthetic and natural polymers such as chitosan could be usefully employed as biomaterials or as low-environmental impact materials. Chitosan is a polysaccharide-type biological polymer. Several advantages can be derived from the use of these macromolecules, for instance good hemocompatibility, low antigenicity and biodegradability suitable for tissue repairing applications. They are non-toxic, show interaction with living cells and behave as multifunctional polymer containing large numbers of reactive amine groups and hydroxyl groups so that they could be used as a tool to modulate the integration into the hosting tissues [20–23]. Chitosan also promotes wound-healing and has bacteriostatic effects [22–24]. It was also observed that when they are blended with synthetic polymers such as poly(vinyl alcohol), they are able to exert a stiffening effect to improve the mechanical properties of the produced materials and to improve its low solubility in water [23]. Finally, chitosan is very abundant, and its production is of low cost and ecologically interesting [22–25].

Another aspect of vital importance on designing materials for bone engineering is associated with the porosity and pore structure of the system. Thus, particular attention has to be paid for the synthesis of bioceramics and composites with porous morphology to allow the in-growth of bone tissue [3,6–12]. The appropriate porosity, pore size distribution and bioactivity allow the adhesion, nucleation and growth of bone tissue to achieve full integration with the living bones. The chemical composition of the tissue engineered scaffold is crucial for the resorbability, osteoconductivity (able to host bone cell) and osteoinductivity (able to induce the formation of bone) with a highly interconnected porous structure together with its internal pore structure for the vascular growth [9,13,16]. Ideally, from the bone tissue engineering design approach, the biomaterial should support compressive loading and tensile or torsion stresses, presenting similar mechanical property compatible with the natural bone tissue [4,6,7,26,27]. Finally, it must also induce cell anchorage and remodel the extracellular matrix in order to integrate with the surrounding tissue. Thus, despite of the complexity of the system, such challenges are yet to overcome in order to achieve proper replacement of bone tissues by synthetic materials [27].

In summary, the present work aimed to synthesize and characterize organic–inorganic hybrids based on PVA modified with different contents of bioactive glass obtained via the sol–gel method and blended with chitosan. The effects of important synthesis parameters such as degree of hydrolysis of PVA and different PVA/bioactive glass (PVA/BaG) composition ratios on the final properties of composites were investigated. Moreover, MTT (3-[4,5-dimetylthiazole-2-yl]-2,5-diphenyltetrazolium bromide) biocompatibility and cytotoxicity assays were also conducted. To our knowledge, this is the first reported research in the literature where 3D porous scaffolds based on tri-component hybrids of PVA, chitosan and bioactive glass (PVA/Chi/BaG) were synthesized and extensively characterized at micro-nanostructure level.

2. Materials and methods

2.1. Synthesis of PVA/bioactive glass (PVA/BaG) and PVA/bioactive glass/chitosan (PVA/BaG/Chi) hybrids

Hybrids containing PVA at three concentrations 80, 70 and 60 wt% and bioactive glass with composition $58SiO_2$–$33CaO$–$9P_2O_5$ were synthesized by foaming a mix-

ture of polymer solution and bioactive glass sol–gel precursor solution and were used for the cytotoxicity and biocompatibility investigation. Two degree of hydrolysis of PVA were used: degree of hydrolysis 98.0–98.8% (Celvol 103, named PVA-98.5), average molecular weight M_w = 13,000–23,000 g/mol and degree of hydrolysis 80% (Aldrich–Sigma, named PVA-80), M_w = 9,000–10,000 g/mol. PVA aqueous solutions were prepared by dissolving the PVA powder in a water bath at 80 °C with a cover glass to minimize evaporation loss, under moderate stirring, for approximately 2 h. PVA aqueous solutions were prepared at concentration of 28 wt% in order to stabilize the foam formation. The starting sol solution was synthesized from mixing tetraethoxysilane (TEOS, Sigma), de-ionized water, triethylphosphate (TEP, Sigma) and calcium chloride ($CaCl_2 \cdot 2H_2O$, Fluka) in presence of hydrochloric acid solution 2N. The molar ratio H_2O/TEOS used was 12:1. To this resulting solution were added the surfactant, sodium lauryl sulphate (SLS), and hydrofluoric acid (HF, Sigma, 10%, v/v solution). The mixture was foamed by vigorous agitation. HF was used to catalyze the gelation. The abrupt change in the rheological behavior was used to identify the gel point [28,29]. The gelation time (T_g) was estimated by visual inspection and was defined as the time interval starting at the moment the addition of HF catalyzer and the instant where no more fluidity could be observed by tilting the reaction vessel at approximately 30°. The foams were cast just before gelation in plastic containers and sealed (cylinder of 20 mm diameter and 30 mm height). Then, the samples were aged and dried at 40 °C for 192 h.

Chitosan hybrid samples (Sigma, high molecular weight, M_w = 161,157 g/mol, viscosity 800–2000 cps, powder, deacetylation degree = 75.6%) were produced by a similar procedure by fully dissolving 2.5 g in 250.0 ml in double-distilled water with 1.0% of HCl (PA, Aldrich) for approximately 4 h at room temperature. Then, the chitosan acidic solution was added to the previously prepared PVA, stirred until a completely homogenous solution was obtained. Then, it was added to the bioactive glass precursors mixture (TEOS:TEP:$CaCl_2$:SLS:HF) at 20 °C and the mixture was vigorously stirred for foaming formation and finally poured into plastic moulds. The PVA/BaG/Chi hybrids were aged and dried at 40 °C for 192 h. Highly uniform tridimensional porous scaffolds were obtained and were further characterized. The molar fractions of reagents used for all composites preparation are presented in Table 1.

2.2. Characterization of PVA/bioactive glass and PVA/chitosan/bioactive glass hybrids

2.2.1. Characterization of structure and morphology

2.2.1.1. Scanning electron microscopy (SEM). SEM images were taken from organic–inorganic hybrids with a JSM 6360LV (JEOL/NORAN) microscope. SEM photomicrographs were used for the evaluation of hybrid foam morphology, microstructure and porosity. Prior to examination, samples were coated with a thin gold film by sputtering. Images of secondary electrons (SE) were obtained using an accelerating voltage of 10–15 kV.

2.2.1.2. Brunauer–Emmett–Teller (BET)method. The BET method was utilized to calculate the specific surface areas. The pore volume and pore size distributions were derived from the adsorption branches of the isotherms. Before measurements, PVA/bioactive glass hybrids were dried at 40 °C for 48 h under N_2 flow. Then, samples were maintained under vacuum for 12 h at 40 °C for proper degassing (Micromeritics). It is important to point out that only mesopore range was evaluated by this method involving N_2 adsorption–desorption isotherms.

2.2.2. Crystallinity and phase characterization by X-ray diffraction

X-ray diffraction characterization (XRD) patterns were obtained from hybrid PVA/BaG and PVA/Chi/BaG samples prepared as crushed powders and films produced from pure polymer precursors of PVA and chitosan (PHILIPS, PW1710) using Cu Kα radiation with λ = 1.54056 Å. XRD analyses were conducted in the 2θ range from 3.03 to 89.91° with steps of 0.06°. Narrow peaks identified within the scan range were confirmed using previously published literature [30,31,34,45,46].

2.2.3. Synchrotron small-angle X-ray scattering characterization (SAXS)

SAXS experiments were carried out on beamline SAS of the National Synchrotron Light Laboratory (LNLS, Campinas, Brazil) by using a fixed wavelength of 0.1488 nm and a sample to detect distance of 1131.2 mm which yield a focused X-ray beam. Bi-dimensional scattering patterns were collected on a CCD camera, and the curve intensities $I(q)$ versus q ($q = 4\pi\sin\theta/\lambda$, where q is the scattering vector, 2θ is the scattering angle and λ the wavelength) were obtained by integrating the data in the

Table 1
Concentration of reagents used for the preparation of PVA/bioactive glass and PVA/chitosan/bioactive glass hybrids H_2O/TEOS = 12

Proportion of phases (wt%) PVA/inorganic phase	PVA degree of hydrolysis (%)	Molar ratio				
		TEOS	TEP	$CaCl_2$	HF	PVA/Chi (%)
60/40	80.0	1.00	0.13	0.61	0.1	–
70/30	80.0				0.2	–
80/20	80.0				0.4	–
60/40	98.5				0.1	–
70/30	98.5				0.2	–
80/20	98.5				0.4	–
70/30	98.5				0.2	0.5

direction of the anisotropic pattern ($1.2 < q < 3.0\,nm^{-1}$). Each SAXS pattern corresponds to a data collection time of 120 s for pure polymers (PVA or chitosan) and 300 s for hybrids. From the experimental scattering intensity produced by all the studied samples, the parasitic scattering intensity was subtracted. All SAXS patterns were treated and corrected by a public domain software for 2D data reduction and analysis (FIT2D, V.V12.077, Hammersley, A.P., ESRF, France), for the time varying intensity of the direct synchrotron beam [30,31,34].

2.2.4. Chemical characterization by FTIR spectroscopy

Fourier transform infrared spectroscopy (FTIR) was used to characterize the presence of specific chemical groups in the PVA, chitosan and PVA-derived hybrid networks. FTIR spectra were obtained within the range between 4000 and 400 cm^{-1} (Perkin–Elmer, Paragon 1000), using the diffuse reflectance spectroscopy method (DRIFTS–FTIR). Hybrid samples were milled and mixed with dried KBr powder (1.0 wt%), then placed in a sampling cup and 64 scans were acquired at 2 cm^{-1} resolution with the subtraction of KBr background. The transmittance FTIR spectrum was also obtained for PVA and chitosan films that were used as a reference.

2.2.5. Characterization of mechanical behavior

The mechanical behavior of the composites was evaluated by compression tests. Specimens were evenly cut from the most homogeneous region of the foam to form blocks measuring 10 mm × 10 mm × 7 mm. These samples were positioned between parallel plates using equipment EMIC DL 3000 and compressed with a crosshead speed of 0.5 mm min^{-1} and a 2.0 kN load cell. At least five samples ($n = 5$) of each composite system were measured and the results averaged. The elastic modulus was calculated as the slope of the initial linear portion of the stress–strain curve. The yield strength was determined from the cross point of the two tangents on the stress–strain curve at the yield point.

2.3. Cytotoxicity and cellular viability activity by MTT assay

Simulated body fluid (SBF) solution [32] was used as a blocking procedure for any remaining cytotoxicity groups from the sol–gel method. So, the porous scaffolds were immersed in 75 ml of acellular SBF solution in polyethylene flasks, with surface area/volume ratio raging from 0.5 to 1.0 cm^{-1}. The flasks were place inside an incubator at controlled temperature of 37 °C for 72 h. Then, the samples were rinsed gently in de-ionized water, and dried at 25 °C for 48 h. All samples subjected to cytotoxicity assay were previously sterilized by exposure to saturated steam of ethylene oxide. The cell viability was assessed by the reduction of the MTT assay using VERO cell monolayers (cell culture isolated from kidney epithelial cells extracted from African green monkey) grown in 96-well microtiter plates. Cell proliferation was measured in 2, 4, 6 and 8 days. MTT reagent was added to each sample and also to the microplate well used as the reference (control) and then incubated at 37 °C for 4 h. Absorbance was read on a microplate reader at wavelength $\lambda = 540$ nm and background (control with no cells) was subtracted from all samples.

3. Results and discussion

3.1. Synthesis of PVA-derived hybrids

Despite of the simplicity of the preparation method the synthesis and process control of inorganic–organic hybrids, produced via sol–gel route, is a rather complex system due to the great number of variables that are usually involved, for instance reagents concentration and miscibility (water, TEOS, TEP and $CaCl_2$), pH changes during the reaction in aqueous medium, proportion ratio between alkoxide precursor and water, temperature, and catalyzer, just to name a few. For that reason, the molar ratio H_2O/TEOS and temperature were kept constant for all experiments. Gelation time is frequently used as a reliable indicative of the overall contribution of processing parameters for products obtained through sol–gel route [12,15,28,29]. In Fig. 1, it is shown the influence in the gelation time by varying the relative PVA (PVA-98.5) concentration in the final PVA/bioactive glass hybrid produced. It can be clearly observed that an increase in PVA content from 0 to 80% (pure BaG and PVA/BaG: 80/20, respectively) has caused a simultaneous increase in the gelation time from approximately 7 min to over 25 min or approximately 400%.

These results can be explained by a closer look to the sol–gel process, as the name implies, usually involves two stages: precursors initially form high molecular weight but still soluble poly-intermediates, a sol, and the intermediates further link

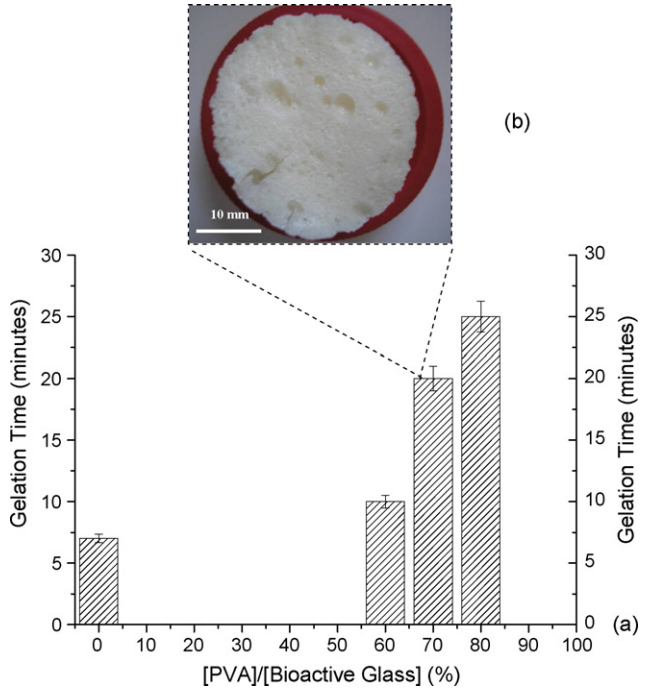

Fig. 1. (a) Effect of PVA concentration on the gelation time for hybrids synthesized (PVA-98.5) and (b) photograph (no magnification) of 3D macroporous scaffold produced.

together to form a three-dimensional network, a gel [28]. Hence, by increasing the PVA concentration in the mixture during the sol–gel reaction, the polymer chain would limit and hinder the interaction among silanol groups of silicates nucleus and polysiloxanes just produced by hydrolysis, causing an increase in the time in the formation of a gel (T_g). Such trend of raising T_g is more pronounced on the PVA with higher degree of hydrolysis (PVA-98.5) than on the low degree (PVA-80, results not showed) due to the formation of hydrogen bonds between hydroxyls from PVA chain and silanol from hydrolyzed alkoxide precursor of SiO_2 (TEOS). On the other hand, PVA-80 presents a higher amount of acetate groups, regulating the extension of interaction of PVA hydroxyls with silanol groups and weakening the hydrogen bonding. As far as the T_g is concerned no significant alteration was detected by adding the chitosan biopolymer to PVA in the molar ratio PVA/chitosan = 0.5%. It was expected that under such diluted concentrations the chitosan would play only a secondary role thus limiting the overall kinetics of the sol–gel processing.

3.2. Characterization of PVA/bioactive glass hybrids

3.2.1. Characterization of structure and morphology by SEM and BET method

SEM characterization was conducted in order to evaluate the porosity, pore morphology and pore size distribution of hybrid scaffolds. SEM micrographs are presented in Fig. 2 (PVA-80%). It was clearly observed that 3D hybrid scaffolds with interconnected macropores typically ranging from 10 to 600 μm were produced by foaming a mixture of PVA aqueous solution and bioactive glass sol–gel precursors, with the aid of the surfactant (SLS).

For the same processing conditions and parameters, there was no detectable variation in the modal macropore diameters of approximately 500 μm and the range of pore size distribution as the content of the inorganic glass phase (BaG) was decreased from 40 to 30 wt%. These hybrid structures with different ratios of PVA/BaG of 60/40 and 70/30 wt% are shown in Fig. 2A–C, respectively. However, there was an unambiguous difference in the morphological aspect between these samples, where a significant qualitative increase in the number of pore ranging from 20 to 100 μm was found for hybrids with higher silica glass content of 40% (PVA/BaG: 60/40, Fig. 2A and B), when compared to lower inorganic phase samples (PVA/BaG: 70/30, Fig. 2C and D). Such difference is attributed to the reduction in flexibility of the organic–inorganic structure formed by increasing the glass content. Thus, the hybrid would be consolidated into a more rigid microstructure during the sol–gel reaction process stabilizing smaller bubbles present in the foam mixture. SEM micrographs of hybrid foam scaffolds produced using PVA blended with chitosan and further reacted to bioactive glass precursors are shown in Fig. 2E–H (PVA/Chi/BaG). Again, despite of a similar macroporous tri-dimensional structure (Fig. 2E), there are some morphological differences when compared to those hybrids of PVA/BaG without chitosan incorporated (Fig. 2A–C). It seems to have lower connectivity on the pore structure that could be explained by the reduction on the foaming effect by the chitosan due to its intrinsic hydrophobic cyclic rings. The SEM micrographs of tri-component scaffold based on PVA/Chi/BaG did not present any evidence of phase segregation or heterogeneity of the hybrid, even at high magnification as it can be observed in Fig. 2G and H. So, hybrid struts with very uniform micro-nanostructure were produced with macropores approximately 500 μm in diameter and interconnected macropore windows with diameters in excess of 100 μm. Although the results obtained by SEM micrographs are quite useful in comparing the macropore structure of the different hybrid materials, and how it is affected by processing and composition, it must be said that they are not absolute values but relative results. An important fact needs to be emphasized in this work that is associated with the crack-free tri-dimensional highly macroporous scaffold that was produced by the novel developed PVA/bioactive glass stoichiometry proportion via sol–gel route. This is a major achievement compared to some papers reported in the literature [12,18,29] where the brittle and fragile behavior of glass derived bioceramic and composites have drastically restricted their application in bone engineering due to the mechanical properties.

In summary, the pore structure obtained is suitable for bone tissue engineering by exhibiting a homogeneous macroporous network with multimodal pore size distribution, namely in the 10–500 μm range, open pores and some interconnectivity. Such hierarchical structure has potential application for future bone tissue in-growth, nutrient delivery to the center of the regenerated tissue and vascularization [6–12].

By varying the ratio of the organic to inorganic phases, we were able to modify the scaffold structural morphology and porosity. All foams exhibited high porosity (P) in the range from 65 to 80%, estimated by using $P = 1 - (\rho/\rho_0)$, where the apparent density (ρ) of the scaffolds was determined by measuring the mass and volume of each scaffold and (ρ_0) is the density of the ideally non-porous material.

The specific surface area of hybrid scaffolds was estimated by the BET method from the nitrogen adsorption–desorption isotherms. The results for the hybrids with composition of 70%PVA–30%BaG have showed that when the PVA with higher hydrolysis degree (98.5%) was used during the synthesis, the average surface area of the scaffold has decreased almost 50%, from 3.0 to 1.6 $m^2\,g^{-1}$, compared to sample with PVA of low degree of hydrolysis (PVA-80.0%). Such effect can attribute to the occurrence of a higher number of hydrogen bonds between hydroxyl groups of PVA chain (PVA-98.5) with the remaining silanol present on the glass surface, causing the formation of a uniform polymer film “capping” the silicates domains. Thus, that would diminish the amount of mesopores in the nanometer scale (2–50 nm). On the other hand, by keeping constant the PVA/BaG ratio and choosing the PVA with lower degree of hydrolysis (PVA-80) the opposite effect is observed. That would represent an increase in the relative number of acetate groups raising the overall surface area due to the formation of mesopores. Thus, the balance of charge of a partially hydrolyzed PVA (PVA-80) would be stabilized by adopting a conformation, where acetate groups are oriented to the center and hydroxyls to the outer part of the molecule in a hydrophilic medium [30,31].

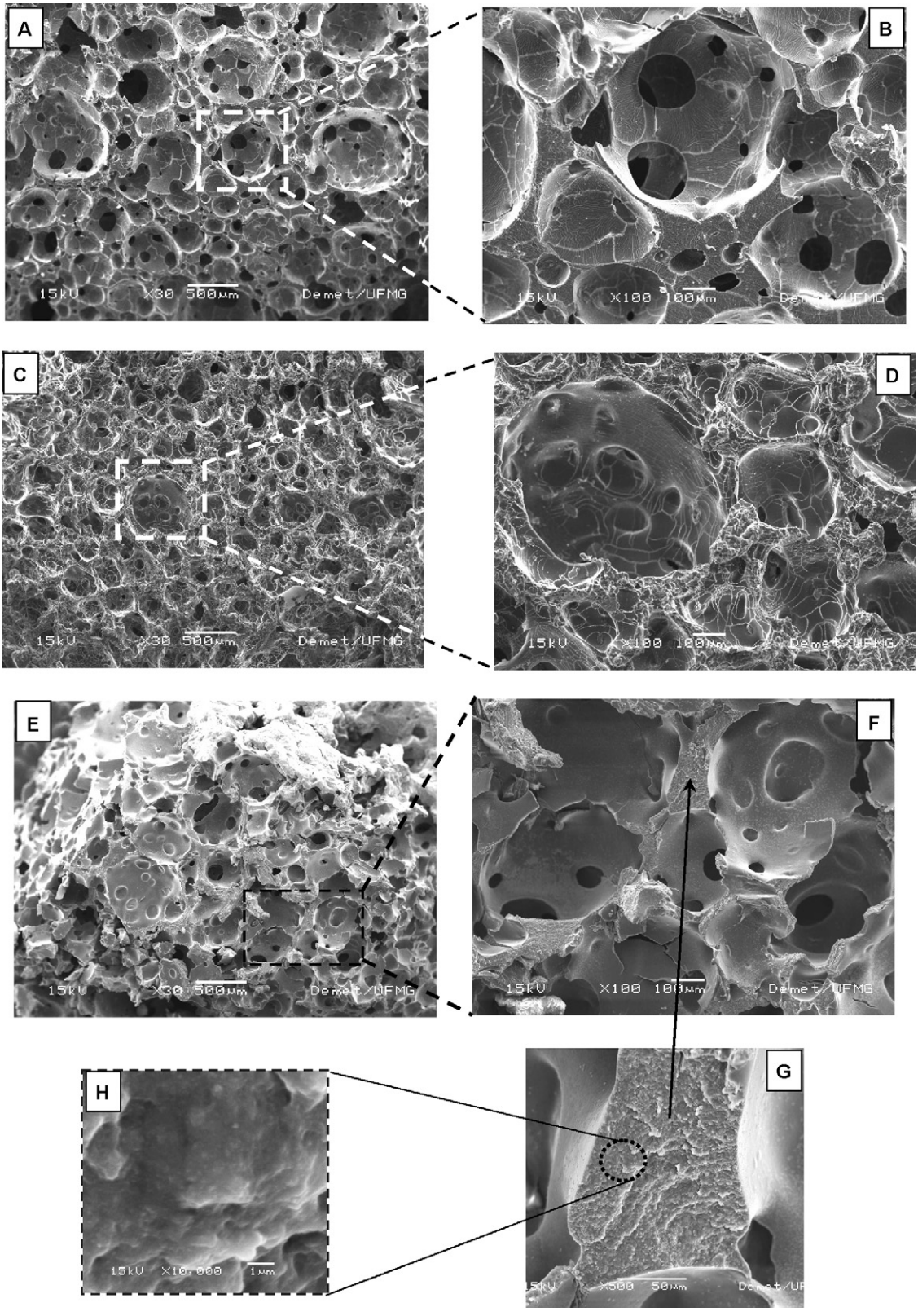

Fig. 2. SEM photomicrographs of hybrids synthesized with PVA-80: (A) PVA/BaG: 60/40, 30×; (b) PVA/BaG: 60/40, 100×; (C) PVA/BaG: 70/30/BaG, 30×; (D) PVA/BaG: 70/30, 100×; (E) PVA/BaG/Chi: 70/30, 30×; (F) PVA/BaG/Chi: 70/30, 100×; (G) PVA/BaG/Chi: 70/30, 500× and (H) PVA/BaG/Chi: 70/30, 10,000×.

Table 2
Major FTIR vibrational bands associated with PVA, chitosan and bioactive glass

Material	Wavenumber (cm^{-1})	Group assignment	References
BaG	461	Si–O–Si stretching	(a)
BaG	822	Symmetric Si–O–Si stretching	(a)
BaG	953	Si–OH bond stretching	(a)
BaG	1000–1220, 960 doublet at $\nu = 569$ and $\nu = 603$	Phosphates (PO_2^-, PO_3^{-2}), (PO_4^{-3})	(a)
BaG	1080	Asymmetric Si–O–Si stretching in SiO_4 tetrahedron	(a)
PVA	1141	C–O stretching, crystallinity	(a)
BaG, PVA	1634	O–H bending (molecular water)	(a)
PVA	2937–2870	CH stretching	(a)
PVA	1710–1740	C=O stretching, acetate groups	(a)
BaG, PVA	3550–3200	O–H stretching and adsorbed water	(a)
Chi	3570–3200	ν OH bonded, ν N–H_2	(b)
Chi	2955–2845	ν C–H (asymmetric)	(b)
Chi	1900–1500	Amide I: νC=O	(b)
Chi	1650–1550, 1570–1515	δN–H (I), δ N–H (II)	(b)
Chi	1650–1550	δN–H (I)	(b)
Chi	1154, 896	ν COC (saccharide- β-1-4)	(b)
Chi	1300–1000	ν C–O (cyclic)	(b)

(a) Refs [30,31,34,36–39] and (b) Refs [40,41].

BET results were used as supporting technique for morphology analysis (SEM). In previous papers of our group [33,34] porosity has been addressed through other methods, based on high bioactive glass content in the hybrid structure formation.

3.2.2. Chemical characterization by FTIR spectroscopy

The main vibrational bands associated with both polymers PVA and chitosan and with the inorganic phase of bioactive glass (BaG, SiO_2–CaO–P_2O_5) are presented in Table 2.

Representative IR spectra of the pure PVA films (PVA-80 and PVA-98.5), the bioactive glass and the hybrid porous scaffold (PVA-80/BaG: 70/30%) are shown in Fig. 3. In Fig. 3a–d, FTIR spectra of pure PVA with different degree of hydrolysis are shown. For both PVA spectra, the broad band observed from 3100 to 3600 cm^{-1} may be assigned to O–H stretching due the strong hydrogen bond of intramolecular and intermolecular type [30,31,36–37]. The presence of a relatively higher

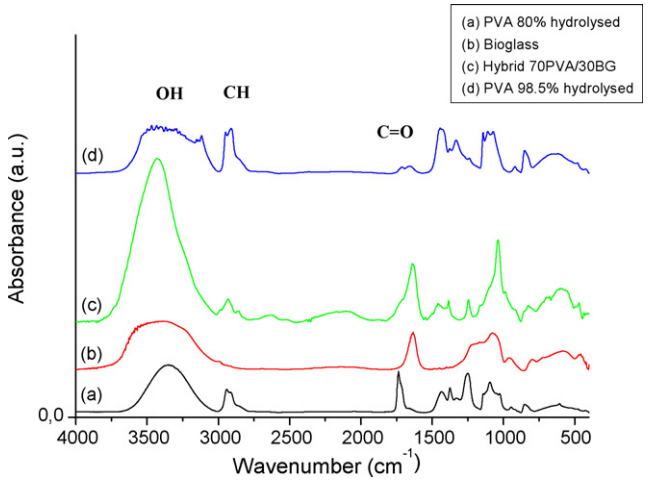

Fig. 3. FTIR spectra of sample: (a) polyvinyl alcohol, PVA-80% hydrolyzed; (b) bioactive glass; (c) hybrid 70 wt%PVA–30 wt%BaG and (d) PVA-98.5% hydrolyzed.

hydroxyl content in the 98.5% hydrolyzed PVA compared to 80% hydrolyzed PVA can be seen from the broader band around 3300 cm^{-1}. The strong band at 2850–2950 cm^{-1} was attributed to alkyl stretching mode (νCH). The absorption band from 1700 to 1750 cm^{-1} arises due to the stretching vibration of carbonyl (C=O) from the acetate group found in partially hydrolyzed PVA polymer and it has a higher relative intensity for the PVA 80% hydrolyzed (Fig. 3a) as expected from remaining acetate groups [30,31,36,37]. The relative crystallinity of two PVA samples with different degree of hydrolysis was verified by the presence of the vibrational band at $\nu = 1141$ cm^{-1} [30,31]. It was noted that PVA with high degree of hydrolysis (PVA-98.5, Fig. 3d) has showed a slight increase in this band when compared to low degree of hydrolysis (PVA-80, Fig. 3a). That means, as the number hydroxyl groups are increased the number of stabilizing hydrogen bonds are simultaneously increased, resulting in a more crystalline polymer network structure [31,36,37]. In the FTIR spectrum of the bioactive glass presented in Fig. 3b the bands related to Si–O–Si asymmetric and symmetric stretching modes are observed at approximately 1080 and 450 cm^{-1}, respectively. A typical absorption band observed in silica gel is located at 1640 cm^{-1} and is attributed to the deformation mode of adsorbed molecular water in the pores [34–37]. The presence of PVA and other polymers in hybrids significantly reduces the possibility of drying and ageing the systems at temperature above 40 °C. Also, the vibrational band at 950 cm^{-1} has been credited to the presence of silanol groups (Si–OH) usually found in silica synthesized via sol–gel method. FTIR spectrum of hybrid with composition of PVA/bioactive glass: 70/30 wt% is presented in Fig. 3c (PVA-80). The bioactive glass component is identified by major vibration bands, (Si–O–Si, at 1080 and 450 cm^{-1}) [30,31]. In addition, the peak at 950 cm^{-1} associated with the Si–OH vibrational mode remains as a shoulder. PVA-derived hybrid samples have also presented broad bands in the frequency ranging from 3000 to 3650 cm^{-1} attributed to both contributions of hydroxyls (PVA) and silanols (BaG) (Fig. 3c). In the range 1500–900 cm^{-1} there is a superposi-

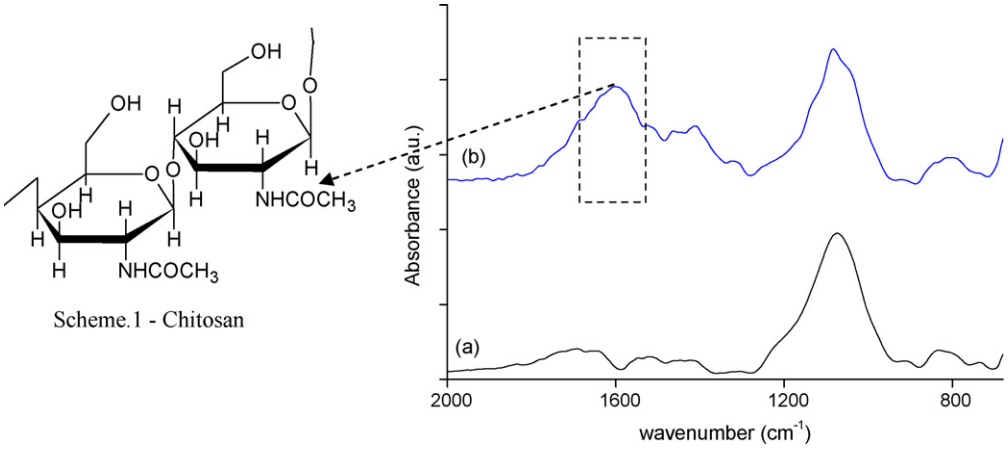

Fig. 4. FTIR spectra of samples synthesized with PVA-80: (a) hybrid of 70 wt%PVA–30 wt% bioactive glass; (b) hybrid of 70 wt%PVA–30 wt% bioactive glass and (b) with 0.5% chitosan (PVA/Chi/BaG); Scheme 1: chemical structure of chitosan biopolymer.

tion of the bands derived from the bioactive glass and the PVA components [31,33,36,37]. Also, typical phosphate group bands at $\nu = 1000$–$1220\,cm^{-1}$ (PO_2^-, PO_3^{2-}) and $\nu = 960\,cm^{-1}$ (PO_4^{3-}). The FTIR spectra of samples containing phosphorus showed a weak signal related to a doublet at approximately $\nu = 565$ and $\nu = 600\,cm^{-1}$, which is associated with the stretching vibrations of phosphate groups related to the presence of crystalline phosphates in the glasses [39,45]. Although not shown in the figures, the spectra of the other hybrids produced with different proportion of PVA/BaG are very similar to the spectra exhibited in Fig. 3c.

FTIR spectra for hybrids of PVA/bioactive glass and PVA, chitosan and BaG are presented in Fig. 4a and b, respectively. It can be observed the contribution of chitosan chemical groups is to the overall hybrid spectrum mainly related to amide groups at vibrational bands ranging from 1000 to $1800\,cm^{-1}$ [18–20,41]. Briefly, in the IR spectrum of chitosan (Fig. 4b), the absorption peak of carbonyl stretching vibration in O=C–NHR groups was observed at approximately $1660\,cm^{-1}$, and the absorption peak at $1590\,cm^{-1}$ was attributed to N–H bending vibration in amine groups [41].

3.2.3. Crystallinity and phase characterization by X-ray diffraction

The X-ray diffraction analysis result from the pure bioactive glass is shown in Fig. 5a. As expected, it did not show the presence of any crystalline phase, being totally amorphous. On the other hand, the XRD patterns from both samples of pure PVA, low degree (PVA-80) and high degree of hydrolysis (PVA-98.5) have shown some diffraction bands (Fig. 5b and c, respectively). Hence, they have both being identified as a semi-crystalline structure, with slightly higher crystallinity for the PVA-98.5 due to the superior concentration of hydroxyls groups (Fig. 7c, Insert). This XRD results have endorsed the previous findings based on FTIR spectrum of PVA with higher degree of hydrolysis (Section 3.2.2). The XRD curve for PVA/bioactive glass hybrid (PVA/BaG: 70/30) synthesized is shown Fig. 7d. It can be directly verified the sum up of both contributions from PVA with semi-crystalline structure and amorphous phase of bioactive glass [34]. In the same way, the hybrid based on PVA/Chi/BaG has presented a diffraction pattern as shown in Fig. 5e. The semi-crystalline structure was maintained when chitosan with acetylation degree of 76% was incorporated to PVA/BaG hybrid. It can be noted three peaks at approximately crystalline peaks at 2θ of 10.3° (1 0 0), 15.2° (0 0 2) and 19.8° (0 2 0), which indicated some degree of crystallinity on the biopolymer network. That would be a typical XRD pattern for the hybrid showing contribution from all components in the system [40,41].

3.2.4. Characterization of PVA hybrids by X-ray scattering

Wide-angle X-ray scattering (WAXS, also called X-ray diffraction) is a powerful tool for understanding crystalline

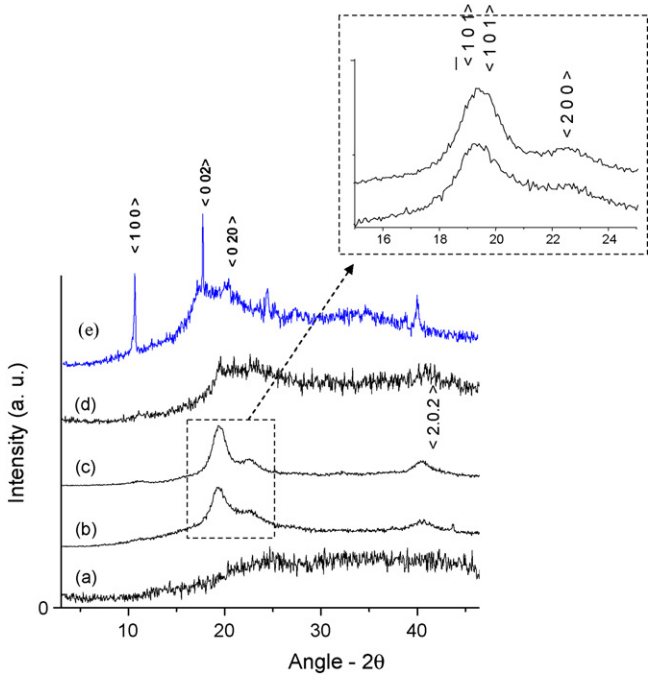

Fig. 5. XRD patterns of (a) bioactive glass SiO_2–CaO–P_2O_5; (b) PVA 80% hydrolyzed; (c) PVA 98.5% hydrolyzed; (d) hybrid 70 wt%PVA–30 wt%BaG and (e) hybrid 70 wt%PVA–30 wt%BaG with chitosan 0.5%; detail: PVA main crystalline peaks.

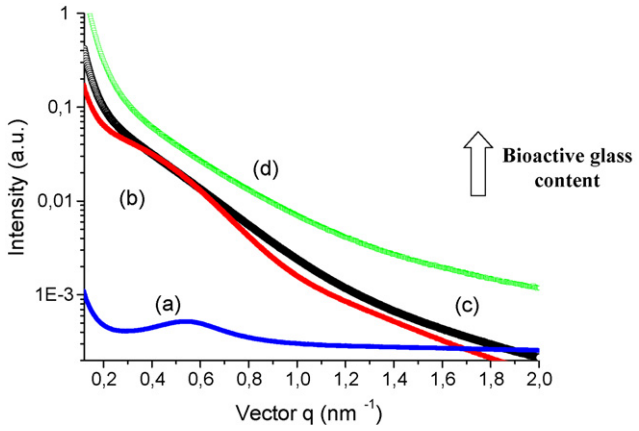

Fig. 6. SAXS studies. SAXS patterns of (a) pure PVA-80, (b) hybrid PVA/BaG: 80/20; (c) hybrid PVA/BaG: 70/30 and (d) pure bioactive glass.

phases, crystal orientations, planes and unit cell structure. Small-angle X-ray scattering is very important to get information from materials structure at the nanometer scale, typically varying from few nanometers to 100 nm [30,31,41]. Synchrotron SAXS curves for pure PVA films and PVA/bioactive glass hybrids are presented in Fig. 6. SAXS results from PVA films have shown a strong single peak with a maximum located at scattering vector (q) 0.54 up to 0.56 nm^{-1} (Fig. 6a). Such trend can be explained by assuming a semi-crystalline structure of PVA polymer sample previously described [30,31]. Considering the conditions of films preparation, that is, PVA crystallized from a dilute solution (5.0 wt%), one would expect that polymer will form lamellar crystals. These crystals are connected to the amorphous regions by polymer chains [30,31]. SAXS curves have indicated a reduction in the peak ($\sim q = 0.55\ nm^{-1}$) as the amount of inorganic phase (BaG) was increased in the samples, from pure PVA (Fig. 6a) to pure bioactive glasses (BaG, Fig. 6d). That is associated with the chemical modification in the original polymer network by a systematically decrease in the crystallinity as the bioactive glass concentration (amorphous) is increased, as verified by FTIR spectroscopy and XRD. Moreover, as the silane coupling reaction mechanism with hydroxyl groups of PVA occurs, it is most likely to reduce the formation of hydrogen bonds and therefore, the driving force for PVA crystallization is also weakened. In other words, the nanostructure of domains was altered by increasing the concentration of inorganic phase to the PVA-derived hybrids [30,31].

Bi-dimensional SAXS images for PVA, PVA/BaG: 80/20, PVA/BaG: 70/30 and BaG are presented in Fig. 7a–d, respec-

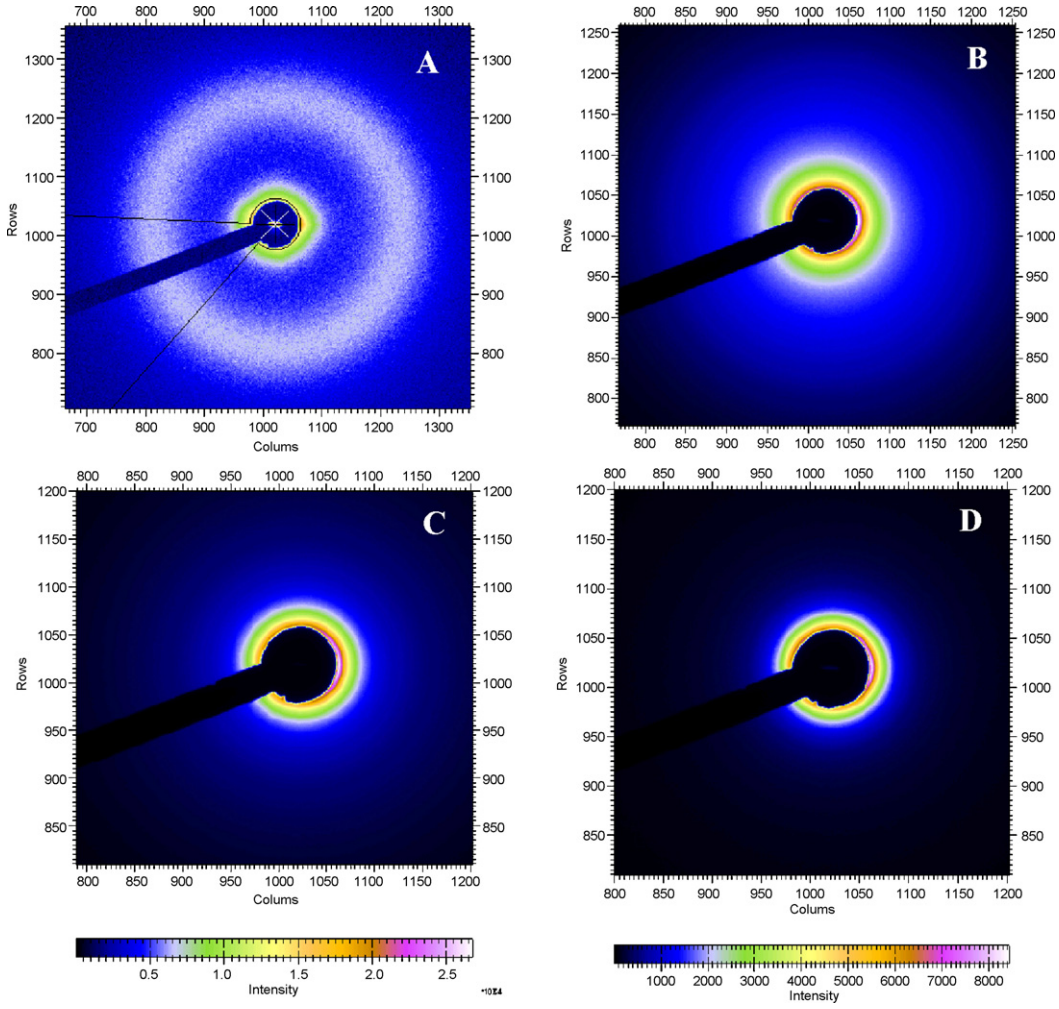

Fig. 7. Two-dimensional SAXS patterns of (a) pure PVA-80, (b) hybrid PVA/BaG: 80/20; (c) hybrid PVA/BaG: 70/30 and (d) pure bioactive glass.

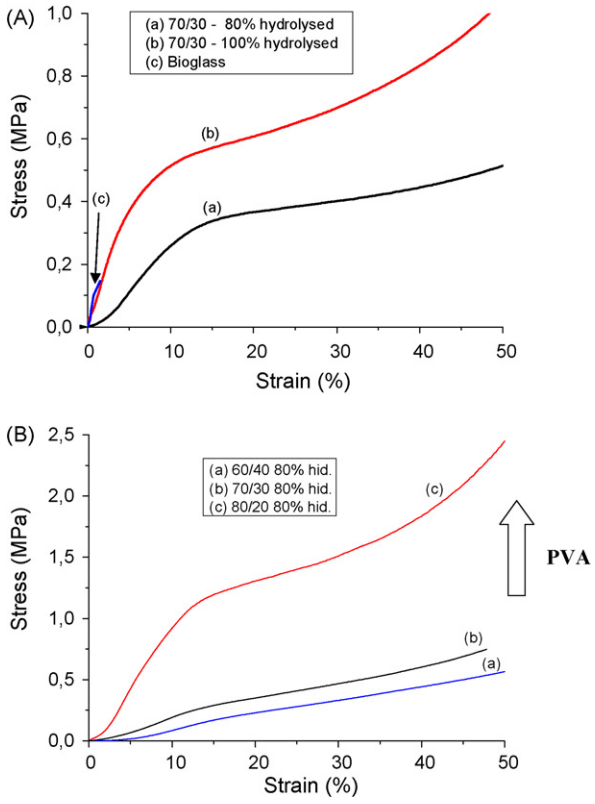

Fig. 8. Stress–strain curves obtained by compression test: (A) PVA/BaG: 70/30 prepared with polymer: curve a, 80% hydrolysis grade; curve b, 98.5% hydrolysis grade and curve c, pure bioactive glass. (B) Hybrids at different concentrations: curve a, PVA/BaG: 80/20; curve b PVA/BaG: 70/30 and curve c PVA/BaG: 60/40.

tively. Again, the scattering patterns have shown strong evidence of reduction in the crystallinity of PVA (Fig. 7a) by raising the BaG content in the hybrids (pure BaG, Fig. 7d). Thus, SAXS results have supported the proposed system of obtaining PVA modified systems at the nanoscale order by incorporating bioactive glass to the newly formed hybrid structure.

3.2.4.1. Characterization of mechanical behavior. The compression tests results of PVA/BaG (PVA/BaG: 70/30 wt%) hybrids are presented in Fig. 8, where PVA-80 is presented in Fig. 8A, curve a and PVA-98.5 in Fig. 8A, curve b. Both curves have shown a similar pattern, with the compressive stress consisted of an initial Hookean region in which stress increased in proportion to strain due to compression of the cell elements followed by a plateau region representing plastic collapse of pores causing densification, with subsequent loading of the cell edges and faces against one to another [42]. The averaged elastic moduli of hybrids were of 2.6 and 6.0 MPa for PVA-80 and PVA-98.5, respectively. These values are in excellent agreement with those values reported in the literature for potential application in repairing cancellous bone tissue [42,43]. The average axial yield strain results were of 11% for hybrids produced with PVA-80 and 6% for PVA-98.5, which is attributed to the effect of crystallinity on the mechanical behavior. As axial yield stress is concerned the values were very similar 0.28 ± 0.02 MPa for hybrids prepared with PVA with different degree of hydrolysis. The organic phase of PVA added to the inorganic phase to produce the hybrid material has advantageously increased the mechanical properties over the pure macroporous bioactive glass usually reported as very fragile and brittle [11,12,33]. It should be emphasized that the PVA-98.5 with higher degree of hydrolysis has presented superior values of all mechanical properties (Fig. 8A, curve b) when compared to PVA-80 (Fig. 8A, curve a), maintaining the PVA/BaG ratio constant. That leads to a very important conclusion, that in fact, the interface PVA/BaG has a stronger interaction of hydroxyls from PVA and silanols from BaG as the degree of hydrolysis is increased. In addition, it is reported in the literature that the higher the degree of hydrolysis of PVA and the polymer M_w the higher are the mechanical properties [33,34]. The effect of increasing of PVA content on the mechanical properties of the hybrid is evidenced by the results shown in Fig. 8B. That is a trend of reducing the brittle behavior of the hybrid by raising the PVA/bioactive glass ratio.

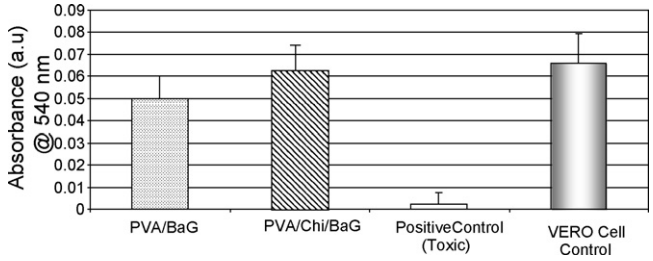

Fig. 9. Relative cell viability of VERO cells cultured with extracts of PVA-80, BaG and hybrid PVA/BaG samples as prepared. Simultaneous cultures were incubated with complete culture medium only as negative control (NC).

Based strictly on these mechanical properties reported, one may assume that the PVA/BaG hybrids developed in the present work are suitable for partial replacement of damaged cancellous bone tissue which has typically a broad range of modulus from 2 to 12 MPa [9,43,44].

3.3. Cytotoxicity and cellular viability activity by MTT assay

The cell viability, bioactivity and cytotoxicity were assessed by the MTT assay and the results are presented in histogram (Fig. 9). The cells treated with extracts of hybrid foams as prepared showed relatively good cell viability compared to the control used as reference. These bioactivity results based on the *in vitro* MTT method have also showed that all experimental groups were not significantly altered either by the PVA/bioactive glass ratio or the degree of hydrolysis of PVA used in the hybrid synthesis. Further investigation is under way where direct contact of cell culture spreading onto PVA/BaG hybrids aiming to mimic the *in vivo* environment of bone tissue replacement.

4. Conclusions

Tri-dimensional porous structures composed of PVA/bioactive glass and PVA/chitosan/bioactive glass were successfully synthesized by the sol–gel route and foaming method. These organic–inorganic hybrid scaffolds exhibited a hierar-

chical structure with interconnected macropores (10–500 μm) and a mesoporous framework typical of gel–glasses (pores of 2–50 nm). By changing the concentration ratio from PVA to bioactive glass and also the degree of hydrolysis from PVA, it was possible to modify the gelation time and, therefore, the resulting foam porosity, pore size distribution and interconnectivity.

FTIR spectroscopy associated with XRD and SAXS have proven to very powerful tools for investigating the formation of PVA/BaG and PVA/Chi/BaG hybrids as organic–inorganic network at micro-nanostructures order.

The increase in the hydrolysis grade of PVA has improved the mechanical properties of the hybrid scaffolds with values suitable for cancellous bone repairing. In addition, the cell viability of all experimental groups was not significantly altered by the PVA/bioactive glass ratio or by incorporating chitosan biopolymer into the hybrid. Hence, it opens a new window of opportunity for developing specially designed materials for biomedical applications.

Acknowledgements

The author acknowledges National Council for Scientific and Technological Development (CNPq) and State of Minas Gerais Research Foundation (FAPEMIG) for financial support on this project. I would like to express my special gratitude to Prof. Dr. Edel F. Barbosa-Stancioli for Microbiology Laboratory and biological assays. Also, the author thanks the important contribution from LNLS staff and for synchrotron SAXS facilities.

References

[1] H.M. Kim, Ceramic bioactivity and related biomimetic strategy, Curr. Opin. Solid State Mater. Sci. 7 (4–5) (2003) 289–299.
[2] B.B. Nissan, Natural bioceramics: from coral to bone and beyond, Curr. Opin. Solid State Mater. Sci. 7 (2003) 283–288.
[3] D. Tadic, F. Beckmann, K. Schwarz, M. Epple, A novel method to produce hydroxyapatite objects with interconnecting porosity that avoids sintering, Biomaterials 25 (2004) 3335–3340.
[4] J.R. Jones, L.L. Hench, Regeneration of trabecular bone using porous ceramics, Curr. Opin. Solid State Mater. Sci. 7 (2003) 301–307.
[5] V. Olivier, N. Faucheux, P. Hardouin, Biomaterial challenges and approaches to stem cell use in bone reconstructive surgery, Drug Discov. Today 9 (2004) 803–811.
[6] K.J.L. Burg, S. Porter, J.F. Kellam, Biomaterial developments for bone tissue engineering, Biomaterials 21 (2000) 2347–2359.
[7] K. Rezwan, Q.Z. Chen, J.J. Blaker, A.B. Boccaccini, Biodegradable and bioactive porous polymer, inorganic composite scaffold for bone tissue engineering, Biomaterials 27 (2006) 3413–3431.
[8] L.L. Hench, Bioceramics: from concept to clinic, J. Am. Ceram. Soc. 74 (1991) 1487–1510.
[9] V.-R. Maria, G.-C. José Maria, Calcium phosphates as substitution of bone tissues, Prog. Solid State Chem. 32 (2004) 1–31.
[10] S. Padilla, S. Sanchez-Salcedo, M. Vallet-Regí, Bioactive glass as precursor of designed-architecture scaffolds for tissue engineering, J. Biomed. Mater. Res. 81A (2007) 224–232.
[11] R.J. Jones, L.M. Ehrenfried, L.L. Hench, Optimizing bioactive glass scaffolds for bone tissue engineering, Biomaterials 27 (2005) 964–973.
[12] M.M. Pereira, J.R. Jones, R.L. Orefice, L.L. Hench, Preparation of bioactive glass-polyvinyl alcohol hybrid foams by the sol–gel method, J. Mater. Sci.: Mater. Med. 16 (2005) 1045–1050.
[13] C. Montserrat, J.S. Antonio, V.-R. María, Amino–polysiloxane hybrid materials for bone reconstruction, Chem. Mater. 18 (2006) 5676–5683.
[14] E. Chiellini, A. Corti, S. D'antone, R. Solaro, Biodegradation of poly(vinyl alcohol) based materials, Prog. Polym. Sci. 28 (2003) 963–1014.
[15] A.P.V. Pereira, L.V. Wander, R.L. Orefice, Novel multicomponent silicate–poly(vinyl alcohol) hybrids with controlled reactivity, J. Non-Cryst. Solids 273 (2000) 180–185.
[16] P. Willi, P.S. Chandra, Nanoceramic matrices: biomedical applications, Am. J. Biochem. Biotechnol. 2 (2) (2006) 41–48.
[17] T. Yamaoka, Y. Tabata, Y. Ikada, Comparison of body distribution of poly(vinyl alcohol) with other water-soluble polymers after intravenous administration, J. Pharmaceut. Pharmacol. 47 (1995) 479–486.
[18] C. Sanchez, F. Ribot, Design of hybrid organic–inorganic materials synthesized via sol–gel chemistry, New J. Chem. 18 (1994) 1007–1047.
[19] Y.-F. Tang, Y.-M. Du, X.-W. Hu, X.-W. Shi, J.F. Kennedy, Rheological characterization of a novel thermosensitive chitosan/poly(vinyl alcohol) blend hydrogel, Carbohydr. Polym. 67 (4) (2007) 491–499.
[20] L.-C. Wang, X.-G. Chen, D.-Y. Zhong, Q.-C. Xu, Study on poly(vinyl alcohol)/carboxymethyl-chitosan blend film as local drug delivery system, J. Mater. Sci.: Mater. Med. 18 (6) (2007) 1125–1133.
[21] S. Yang, K.-F. Leong, Z. Du, C.-K. Chua, The design of scaffolds for use in tissue engineering. Part I. Traditional factors, Tissue Eng. 7 (6) (2001) 679–689.
[22] M.G. Cascone, N. Barbani, C. Cristallini, P. Giusti, G. Ciardelli, L. Lazzeri, Bioartificial polymeric materials based on polysaccharides, J. Biomater. Sci. Polym. Edn. 12 (3) (2001) 267–281.
[23] Y.-L. Liu, Y.-H. Su, J.-Y. Lai, In situ crosslinking of chitosan and formation of chitosan–silica hybrid membranes with using γ-glycidoxypropyltrimethoxysilane as a crosslinking agent, Polymer 45 (2004) 6831–6837.
[24] J. Bergera, M. Reist, J.M. Mayer, O. Felt, R. Gurny, Structure and interactions in chitosan hydrogels formed by complexation or aggregation for biomedical applications, Eur. J. Pharmaceut. Biopharmaceut. 57 (2004) 35–52.
[25] J. Berger, M. Reist, J.M. Mayer, O. Felt, N.A. Peppas, R. Gurny, Structure and interactions in covalently and ionically crosslinked chitosan hydrogels for biomedical applications, Eur. J. Pharmaceut. Biopharmaceut. 57 (2004) 19–34.
[26] M.M. Pereira, A.E. Clark, L.L. Hench, Calcium-phosphate formation on sol–gel-derived bioactive glasses in-vitro, J. Biomed. Mater. Res. 28 (1994) 693.
[27] V.-R. María, Revisiting ceramics for medical applications, Dalton Trans. (2006) 5211–5220.
[28] C.J. Brinker, G.W. Scherer, Sol–Gel Science: The Physics and Chemistry of Sol–Gel Processing, Academic Press, New York, NY, 1990.
[29] A. Oki, X. Qiu, O. Alawode, B. Foley, Synthesis of organic–inorganic hybrid composite and its thermal conversion to porous bioactive glass monolith, Mater. Lett. 60 (2006) 2751–2755.
[30] H.S. Mansur, R.L. Oréfice, A.A.P. Mansur, Characterization of poly(vinyl alcohol)/poly(ethylene glycol) hydrogels and PVA-derived hybrids by small-angle X-ray scattering and FTIR spectroscopy, Polymer 45 (2004) 7193–7202.
[31] G. Andrade, E.F. Barbosa-Stancioli1, A.A. Piscitelli Mansur, W.L. Vasconcelos, H.S. Mansur, Design of novel hybrid organic–inorganic nanostructured biomaterials for immunoassay applications, Biomed. Mater. 1 (2006) 221–234.
[32] T. Kokubo, Apatite formation on surfaces of ceramics, metals and polymers in body environment, Acta Mater. 46 (1998) 2519–2527.
[33] M.M. Pereira, J.R. Jones, L.L. Hench, Bioactive glass and hybrid scaffolds prepared by sol–gel method for bone tissue engineering, Adv. Appl. Ceram. 104 (1) (2005) 35–42.
[34] H.S. Costa, G.I. Andrade, E.F. Barbosa-Stancioli, M.M. Pereira, R.L. Orefice, H.S. Mansur, Sol–gel derived composite from bioactive glass–polyvinyl alcohol, J. Mater. Sci. 43 (2008) 494–502.
[35] W. Tao, T. Mahir, S. Gunasekaran, Selected properties of pH-sensitive, biodegradable chitosan–poly(vinyl alcohol) hydrogel, Polym. Int. 53 (2004) 911–918.

[36] H.S. Mansur, R.L. Oréfice, W.L. Vasconcelos, Z.P. Lobato, L.J. Machado, Biomaterial with chemically engineered surface for protein immobilization, J. Mater. Sci.: Mater. Med. 16 (2005) 333–340.
[37] J. Coates, in: R.A. Meyers (Ed.), Encyclopedia of Analytical Chemistry: Interpretation of Infrared Spectra, a Practical Approach, John Wiley and Sons Ltd., Chichester, 2000, pp. 10815–10837.
[38] R.M. Almeida, C.G. Pantano, Structural investigation of silica gel films by infrared spectroscopy, J. Appl. Phys. 68 (1990) 1225–1232.
[39] J. Román, S. Padilla, M. Vallet-Regí, Sol–gel glasses as precursors of bioactive glass ceramics, Chem. Mater. 15 (2003) 798–806.
[40] Y. Zhang, Preparation of electrospun chitosan/poly(vinyl alcohol) membranes, Colloid Polym. Sci. 285 (2007) 855–863.
[41] S.S. Silva, Functional nanostructured chitosan–siloxane hybrids, J. Mater. Chem. 15 (2005) 3952–3961.
[42] L.J. Gibson, Biomechanics of cellular solids, J. Biomech. 38 (2005) 377–399.
[43] D. Shi, G. Jiang, Synthesis of hydroxyapatite films on porous Al_2O_3 substrate for hard tissue prosthetics, Mater. Sci. Eng. C 6 (1998) 175–182.
[44] M.O. Montjovent, L. Mathieu, B. Hinz, L.L. Applegate, P.E. Bourban, P.Y. Zambelli, J.A. Manson, D.P. Pioletti, Biocompatibility of bioresorbable poly(L-lactic acid) composite scaffolds obtained by supercritical gas foaming with human fetal bone cells, Tissue Eng. 11 (2005) 1640–1649.
[45] A.I. Martin, A.J. Salinas, M. Vallet-Regi, Bioactive and degradable organic–inorganic hybrids, J. Eur. Ceram. Soc. 25 (2005) 3533–3538.
[46] J.D. Cho, W.S. Lyoo, S.N. Chvalun, J. Blackwell, X-ray analysis and molecular modeling of poly(vinyl alcohol)s with different stereoregularities, Macromolecules 32 (1999) 6236–6241.